Novel methods for improvement of a Penning ion source for neutron generator applications[a)]

A. Sy,[1,2,b)] Q. Ji,[1] A. Persaud,[1] O. Waldmann,[1] and T. Schenkel[1]
[1]*Lawrence Berkeley National Laboratory, 1 Cyclotron Road, Berkeley, California 94720, USA*
[2]*Department of Nuclear Engineering, University of California, Berkeley, Berkeley, California 94720, USA*

(Presented 12 September 2011; received 12 September 2011; accepted 27 October 2011; published online 14 February 2012)

Penning ion source performance for neutron generator applications is characterized by the atomic ion fraction and beam current density, providing two paths by which source performance can be improved for increased neutron yields. We have fabricated a Penning ion source to investigate novel methods for improving source performance, including optimization of wall materials and electrode geometry, advanced magnetic confinement, and integration of field emitter arrays for electron injection. Effects of several electrode geometries on discharge characteristics and extracted ion current were studied. Additional magnetic confinement resulted in a factor of two increase in beam current density. First results indicate unchanged proton fraction and increased beam current density due to electron injection from carbon nanofiber arrays. © *2012 American Institute of Physics*. [http://dx.doi.org/10.1063/1.3670744]

I. INTRODUCTION

Penning ion sources[1–3] have long been used for neutron generation through D-D or D-T fusion reactions due to their low power consumption, ease of operation, and ability for compactness. Maximum neutron yields are limited by the poor atomic ion fraction characteristic of Penning discharges; typically over 90% of extracted ions are molecular, necessitating high beam energy and current to obtain suitable neutron yields for imaging and interrogation purposes. For a hydrogen discharge, the poor proton fraction has been attributed to low electron density and short dwell time of molecular hydrogen (H_2^+) ions.[4] Deuterium discharges are expected to behave in a similar manner. Increased neutron yields can be directly expected from increased electron density in the discharge, as both atomic ion fraction and ion density should increase with increased electron density.

We have fabricated a Penning source (Figure 1) for implementation of novel methods of improvement of the electron density in a hydrogen discharge. The cylindrical plasma volume is 2.54 cm in diameter and 3.14 cm in length, bounded radially by the anode and axially by two separate cathodes. A positive bias with respect to the cathode is applied to the anode to maintain the discharge. The axial magnetic field characteristic of Penning sources is generated by an external field coil. The modular nature of the fabricated source allows for the effects of different configurations on proton fraction and beam current to be observed.

II. METHODS

A. Wall material optimization

Several materials were investigated for use as plasma-facing materials for enhanced source operation; the effects of aluminum, molybdenum, gold, graphite, and platinum electrodes on discharge characteristics were observed. The effect of boron nitride as a cathode covering material was also observed; boron nitride enhances the proton fraction in hydrogen ion sources due to its low hydrogen atom recombination coefficient.[5] An ideal electrode material would have a high secondary electron emission coefficient under both ion and electron bombardment and would also inhibit recombination effects that may occur through plasma-wall interactions. Materials with low electron work functions are expected to produce stronger discharge characteristics. Material effects were observed using interchangeable electrodes of the materials studied; each test utilized electrodes of a single material. Baseline operation of the source was characterized using aluminum electrodes.

B. Electrode geometry

Several electrode configurations were implemented to observe the effects of electrode geometry on discharge characteristics. The original configuration featured smooth cathodes and a 2.54 cm long anode. A grooved aluminum cathode and "long" aluminum anode, 4.1275 cm long, were implemented separately for comparison with the original configuration. The grooved aluminum cathode featured 1 mm wide, 0.5 mm deep concentric grooves that increased the cathode surface area by a factor of two. The "long" aluminum anode increased the discharge volume by a factor of 1.5875.

C. Multi-cusp magnetic confinement

Multi-cusp magnetic fields improve the plasma density through improved confinement of primary ionizing electrons.[6] Multi-cusp magnetic field lines extend into the discharge region and reflect electrons back into the plasma, increasing the lifetime of ionizing electrons by reducing electron losses to the anode. The multi-cusp magnetic field was

[a)]Contributed paper, published as part of the Proceedings of the 14th International Conference on Ion Sources, Giardini Naxos, Italy, September 2011.
[b)]Electronic mail: asy@lbl.gov.

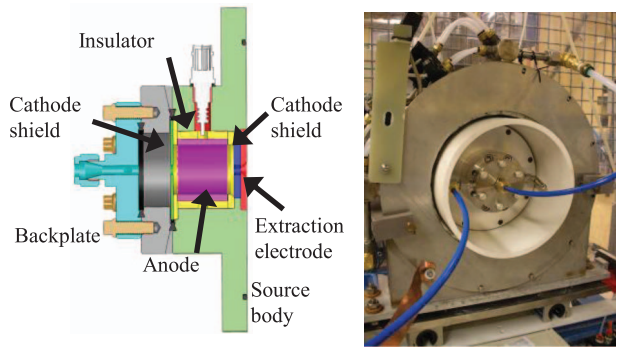

FIG. 1. (Color online) Schematic of Penning source (l) and photo of Penning source mounted on teststand (r).

implemented with NdFeB permanent magnets; the multi-cusp magnets superimpose the resultant radial field distribution over the existing axial magnetic field. Figure 2 shows a Pandira simulation of the radial magnetic field distribution and the actual multi-cusp magnet configuration. Multi-cusp magnetic confinement was implemented with aluminum, platinum, and gold electrodes, as well as with the long aluminum anode.

D. Electron injection with field emitter arrays

Field emitter arrays were integrated into the source for electron injection into the discharge. Carbon nanofiber arrays[7] were mounted on the cathode shield near the backplate within the Penning source for electron injection along the axial direction, towards the extraction electrode; a grid placed between the field emitter arrays and the anode provided the field necessary for electron emission.

III. RESULTS AND DISCUSSION

Table I lists the measured ion fractions obtained from hydrogen discharges during operation with various electrode materials; most discharges were ignited and maintained with 0.8 mTorr source pressure, 800 V applied anode voltage, and 410 G axial magnetic field. Stable operation with boron nitride required slightly higher pressure and discharge voltage. Typical proton fractions fell in the range of 5%–10%; the addition of boron nitride as an effective cathode resulted in a factor of two increase in the proton fraction when compared to baseline operation with aluminum. Figure 3 shows the beam current density as a function of beam energy; beam current density values for beam energy of 3 keV are also listed in Table I. It is noted that the beam current density tends to decrease for beam energies greater than 3 keV due to use of an extraction system not optimized for this ion source. Most materials outperformed the baseline case with aluminum electrodes, likely the result of larger secondary electron emission coefficients;[8] operation with gold and platinum electrodes resulted in a factor of two increase in beam current density. Operation with boron nitride resulted in a factor of three decrease in the beam current density.

TABLE I. Ion fractions and beam current density for discharges with various electrode materials. Beam current density given for beam energy of 3 keV.

	H^+ (%)	H_2^+ (%)	H_3^+ (%)	Beam current density (μA/cm^2)
Aluminum	6.9	92.8	0.3	110.9
Molybdenum	6.3	93.3	0.4	145.9
Gold	7.7	91.3	1.0	219.2
Graphite	8.0	91.5	0.5	185.7
Platinum	8.9	90.1	1.0	229.4
Aluminum with boron nitride	16.2	80.4	3.4	79.5

The increased surface area of the grooved cathode had no effect on the beam current density; operation with the long anode resulted in a factor of three increase in the beam current density. Electrons in the discharge are confined to oscillate between the two cathodes; increasing the anode length increases the distance that electrons travel between the two cathodes, and more ionization can occur for a given pass through the discharge.

The effect of multi-cusp magnetic confinement on the beam current density can be seen in Figure 4. For discharges with the original anode length, the extracted ion current increased by as much as a factor of three with the additional magnetic confinement. Combining the long anode with multi-cusp magnets for aluminum electrodes resulted in an overall increase by a factor of eight over the baseline case. It is anticipated that combining multi-cusp magnetic confinement with increased length of the discharge region will result in further

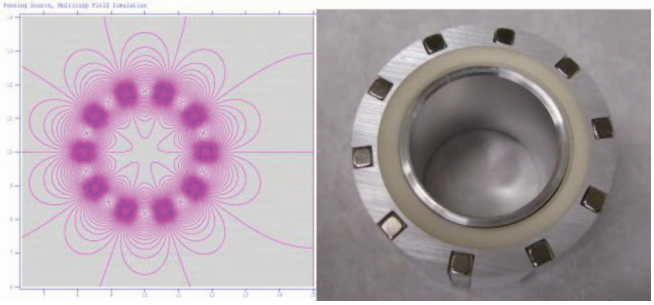

FIG. 2. (Color online) Simulated multi-cusp magnetic field (l) and photo of actual multi-cusp magnets, insulator, and anode (r). The simulated multi-cusp magnetic field is strongest near the inner wall of the anode, with a magnitude of 650 G. The outer diameter of the anode is 2.54 cm.

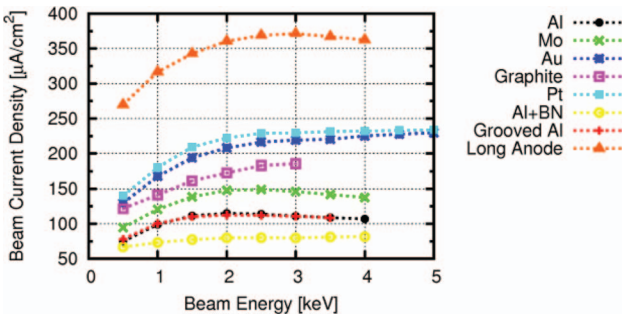

FIG. 3. (Color online) Beam current density for various electrode material and geometry configurations.

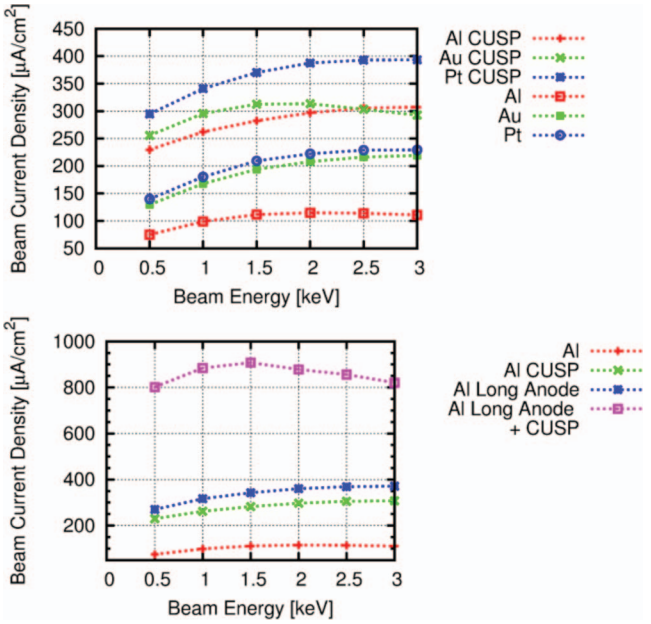

FIG. 4. (Color online) Beam current density with and without multi-cusp magnetic confinement.

improvement to the extracted ion current for discharges with gold and platinum electrodes.

Electron current as a function of the electric field applied to the carbon nanofiber arrays was measured to characterize electron injection into the discharge. Electron currents of up to 30 μA were measured from the carbon nanofiber arrays when no plasma was present. Up to 250 nA of electron current was injected into the hydrogen discharge; injected current values were assumed based on the applied field and previously measured electron emission data. Electrons were injected into the discharge with energies up to 300 eV. Discharge instabilities were observed when the injected electron current exceeded 1 μA. No significant effect on the proton fraction in the discharge was observed due to electron injection. The effect of electron injection on the beam current density can be seen in Figure 5. Increased injected electron current is accompanied by increased ion current density, but it is noted that other processes may be at play during operation with the field emitter arrays as the total discharge voltage increases with increasing emission.

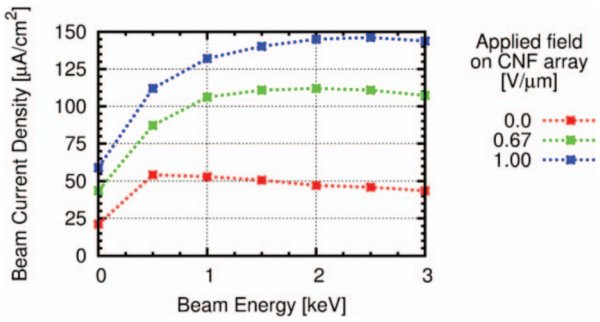

FIG. 5. (Color online) Beam current density with and without electron field emission.

IV. SUMMARY AND FUTURE WORK

Simple modifications to a Penning ion source, including material and geometry optimization as well as multi-cusp magnetic confinement, result in up to an eightfold increase in the extracted ion current. Preliminary results indicate that electron injection into the discharge increases the beam current density. The instability of the discharge due to electron injection is under investigation. Implementation of field emitter arrays with multi-cusp magnetic confinement will be explored.

ACKNOWLEDGMENTS

The authors would like to thank Michael Dickinson and Steve Wilde for their technical support, as well as Rehan Kapadia and Kuniharu Takei for fabrication of the field emitter arrays. This work was performed under the auspices of the U.S. Department of Energy (DOE), NNSA Office of Nonproliferation Research and Engineering NA-22 by Lawrence Berkeley National Laboratory (Contract No. DE-AC02-05CH11231).

[1] J. L. Rovey, B. P. Ruzic, and T. J. Houlahan, Rev. Sci. Instrum. **78**, 106101 (2007).
[2] B. K. Das and A. Shyam, Rev. Sci. Instrum. **79**, 123305 (2008).
[3] J. R. J. Bennett, IEEE Trans. Nucl. Sci., **19**, 48 (1972).
[4] F. K. Chen, J. Appl. Phys. **56**, 3191 (1984).
[5] T. Taylor and J. S. C. Wills, Nucl. Instrum. Methods Phys. Res. A **309**, 37 (1991).
[6] K. N. Leung, T. K. Samec, and A. Lamm, Phys. Lett. **51A**, 490 (1975).
[7] A. Persaud, I. Allen, M. R. Dickinson, T. Schenkel, R. Kapadia, K. Takei, and A. Javey, J. Vac. Sci. Technol. B **29** 02B107 (2011).
[8] *CRC Handbook of Chemistry and Physics*, 91st ed. (CRC Press: Boca Raton, FL, 2011), pp. 12–115.